HIGH ENERGY PHENOMENA IN MASSIVE STARS
ASP Conference Series, Vol. 422, © 2010
J. Martí, P. L. Luque-Escamilla, and J. A. Combi, eds

On the Shape of the Spectrum of Cosmic-Rays Protons produced inside Superbubbles

Gilles Ferrand

Irfu, Service d'Astrophysique, Orme des Merisiers, CEA-Saclay, 91191 Gif-sur-Yvette Cedex, France

Alexandre Marcowith

Laboratoire de Physique Théorique et Astroparticules, CNRS, Université Montpellier II, Place Eugène Bataillon, 34095 Montpellier, Cédex, France

Abstract. In this work we investigate the shape of the spectrum of cosmic ray (CR) protons produced inside superbubbles (SB), by the means of a simple semi-analytical model of CR production and transport embedded inside Monte-Carlo simulations of OB associations timelines. We consider regular acceleration (Fermi I process) at the shock front of supernova remnants (SNRs), as well as stochastic re-acceleration (Fermi II process) and escape controlled by magnetic turbulence inside the SB. In this first attempt we limit ourselves to linear acceleration by strong shocks and neglect protons energy losses. We observe that CR spectra, although strongly intermittent, get a distinctive shape resulting from a competition between acceleration and escape: they are harder at the lowest energies (slope $s < 4$) and softer at the highest energies ($s > 4$). The momentum at which this spectral break occurs depends critically on the various SB parameters - but interestingly all their effects can be summarized by a single dimensionless parameter. For reasonable values of SB parameters, and especially for highly magnetized and turbulent SBs, very hard spectra can be obtained over an important range of CR energies, which has important implications on the high-energy emission from these objects.

Introduction

Our aim is to investigate the average shape of the spectrum of CR protons produced inside SBs. To do so we embed semi-analytical models of CR acceleration and transport inside Monte-Carlo simulations of OB clusters timelines.

1. OB Clusters: Random Samplings of Supernovae

We are interested here in massive stars which die by core-collapse, producing type Ib, Ic or II supernovae, that is of mass greater than $m_{\min} = 8\,m_\odot$, and up to say $m_{\max} = 120\,m_\odot$. These are stars of spectral type O ($> 20\ m_\odot$) and part of stars of spectral type B ($4 - 20\ m_\odot$). Most massive stars spend all their life within the cluster in which they were born, forming so-called OB associations. In order to describe the evolution of such a cluster, one needs to know the distribution of star masses and lifetimes.

1.1. Distribution of Stars

Distribution of Masses The Initial Mass Function (IMF) ξ is defined so that the number of stars in the mass interval m to $m+\mathrm{d}m$ is $\mathrm{d}n = \xi\,(m) \times \mathrm{d}m$, so that the number of stars of masses between $m_{\min}$ and $m_{\max}$ is $N_\star = \int_{m_{\min}}^{m_{\max}} \xi\,(m)\ \mathrm{d}m$. Observations show that ξ can be expressed as a power-law (Salpeter 1955): $\xi\,(m) \propto m^\alpha$, with an index of $\alpha = 2.30$ for massive stars (Kroupa 2002).

Distribution of Lifetimes The more massive they are, the faster stars burn their material. Stars lifetimes can be computed from stellar evolution models, we use here data from Limongi & Chieffi (2006). A star at the threshold $m_{\min} = 8\,m_\odot$ has a lifetime of $t_{\mathrm{SN,max}} \simeq 37\,\mathrm{Myr}$, which is also the total lifetime of the cluster, a star of $m_{\max} = 120\,m_\odot$ lives only $t_{\mathrm{SN,min}} \simeq 3\,\mathrm{Myr}$. Regarding supernovae, the active lifetime of the cluster is thus $\Delta t^\star_{\mathrm{OB}} = t_{\mathrm{SN}}\,(m_{\min}) - t_{\mathrm{SN}}\,(m_{\max}) \simeq 34\,\mathrm{Myr}$.

1.2. Distribution of Supernovae

We are now able to re-construct the story of any given cluster. In order to work out the average properties of a cluster of $N_\star$ stars, we perform random samplings in the IMF. As an illustration of this Monte-Carlo procedure, if we sample the lifetime of each cluster by small enough time-steps (of say $\mathrm{d}t = 10^5$ yr) and count the number n_{SN} of supernovae in each time bin $[t, t+\mathrm{d}t]$, we get an estimate of the mean SN rate as $n_{\mathrm{SN}}\,(t)\,/\mathrm{d}t$. In agreement with Cerviño et al. (2000), we observe that the distributions of masses and lifetimes combine in such a way that, but for a peak at the beginning, the rate of SNs is fairly constant during the cluster's life, and can be expressed as a first approximation as $\mathrm{d}n_{\mathrm{SN}}/\mathrm{d}t \simeq N_\star/\Delta t^\star_{\mathrm{OB}} \simeq N_\star \times 3.10^{-8}\ \mathrm{yr}^{-1}$.

2. Supernovae Shocks: Regular Acceleration

Galactic CRs are believed to be produced at SNRs through diffusive shock acceleration (DSA), a first order Fermi process powered by the velocity divergence of the shock and made possible by the scattering off magnetic turbulence.

2.1. Green Function

To keep things as simple as possible, we limit ourselves here to the test-particle approach. In this linear regime, we know the Green function G_1 which links the CR distributions[1] downstream and upstream of a single shock as

$$f_{\mathrm{down}}\,(p) = \int_0^\infty G_1\,(p, p_0)\ f_{\mathrm{up}}\,(p_0)\ \mathrm{d}p_0\,. \tag{1}$$

to be

$$G_1\,(p, p_0) = \frac{s_1}{p_0}\left(\frac{p}{p_0}\right)^{-s_1} H\,(p - p_0) \tag{2}$$

where H is the Heaviside function and $s_1 = 3r/r - 1$.

[1] $f(p)$ is defined so that the density is $n = \int_p f\,(p)\ 4\pi p^2\ \mathrm{d}p$, where p is the particle momentum.

Mono-energetic injection of CRs at the shock front leads to a power law spectrum[2].

2.2. Multiple Acceleration

As massive stars live in groups, SNs are correlated in space and time. Hence we consider the possibility of multiple acceleration, that is CRs produced by a SN shock being re-accelerated by subsequent SN shocks before they escape the SB.

The effect of repeated acceleration is basically to harden the spectra (Achterberg 1990, Melrose & Pope 1993). The spectrum is no longer a power-law, but one can show that in the limit of an infinity of shocks it reduces again to a simple power-law of slope $s = 3$ (without considering losses and escape).

Note that, when dealing with multiple shocks, it is mandatory to account for adiabatic decompression between shocks: CRs bound to the fluid will be see their momenta decreased by a factor $R = r^{1/3}$ when the fluid density is decreased by a factor r. In order to resolve decompression properly the numerical momentum resolution $\mathrm{d}\log p$ has to be significantly smaller than the induced momentum shift (Ferrand, Downes, & Marcowith 2008).

3. Magnetic Turbulence: Stochastic Acceleration and Escape

CRs accelerated by SNR shocks, although very energetic, might remain for a while inside the SB because of magnetic turbulence which scatters them (they perform a random walk until they escape at the boundaries). Because of this turbulence, CRs will also experience stochastic re-acceleration (second order Fermi process) during their stay in the SB.

3.1. Diffusion Scales

The turbulent magnetic field δB is represented through its power spectrum $W(k)$, defined so that $\delta B^2 \propto \int_{k_{\min}}^{k_{\max}} W(k)\,\mathrm{d}k$ with $k = 2\pi/\lambda$ where λ is the turbulence scale. This spectrum is usually taken to be a power-law of index q:

$$W(k) \propto k^{-q}\,, \tag{3}$$

normalised through the turbulence level $\eta_T = \langle \delta B^2 \rangle / \left(B^2 + \langle \delta B^2 \rangle \right)$.

Space Diffusion If turbulence follows (3) then the diffusion coefficient reads

$$D_x\left(p\right) = D_x^\star \times \left(\frac{p}{m_p c} \right)^{2-q} \tag{4}$$

---

[2]Accelerated particles may back-react on their accelerator, modifying the shock structure and thus the way they are accelerated, which produces concave spectra (e.g. Malkov & Drury 2001). We will explore this non-linear regime in a subsequent work, using our numerical code for the time-dependent simulation of diffusive shock acceleration (Ferrand, Downes, & Marcowith 2008). and/or the stationary semi-analytical model of Blasi (2002), the index of which is controlled by the shock compression ratio only, and is always $s = 4$ in the limit of strong shocks $r = 4$.

with (using results from Casse, Lemoine, & Pelletier (2002) for isotropic turbulence)

$$D_x^\star \propto \eta_T^{-1}\ B^{q-2}\ \lambda_{\rm max}^{q-1}\,. \tag{5}$$

Escape Particles diffuse over a typical length $x_{\rm diff} = \sqrt{6\ D_x\ t}$. They are confined in the acceleration region of size $x_{\rm acc}$ as long as $x_{\rm diff}\,(t) < x_{\rm acc}$, hence a typical escape time $t_{\rm esc} = x_{\rm acc}^2/6\ D_x$, that is using (4)

$$t_{\rm esc}\,(p) = t_{\rm esc}^\star \times \left(\frac{p}{m_p c}\right)^{q-2} \tag{6}$$

with

$$t_{\rm esc}^\star \propto \eta_T\ B^{2-q}\ \lambda_{\rm max}^{1-q}\ x_{\rm acc}^2\,. \tag{7}$$

Acceleration Interaction with waves also leads to a diffusion in momentum. Using results from quasi-linear theory we can express the diffusion coefficient as

$$D_p\,(p) = D_p^\star \times (m_p c)^2 \times \left(\frac{p}{m_p c}\right)^q \tag{8}$$

with

$$D_p^\star \propto \eta_T\ B^{4-q}\ \lambda_{\rm max}^{1-q}\ n^{-1}\,. \tag{9}$$

where n is the number density.

3.2. Green Function

Becker, Le, & Dermer (2006) have recently given the first analytical expression of the Green function G_2 for both Fermi 2 acceleration and escape, valid for any turbulence index $q \in]0,2[$. It is defined so that, for impulsive injection of distribution $f_{\rm init}$, the distribution after time t is

$$f_{\rm end}\,(p,t) = \int_0^\infty G_2\,(p,p_0,t)\ \ f_{\rm init}\,(p_0)\ \,{\rm d}p_0\,. \tag{10}$$

Neglecting losses[3] it can be expressed as

$$\begin{aligned} G_2\,(p,p_0,t) &= \frac{2-q}{p_0}\,\sqrt{\frac{p}{p_0}}\,\frac{\sqrt{z z_0 \xi}}{1-\xi} \\ &\times \exp\left(-\frac{(z+z_0)\,(1+\xi)}{2\,(1-\xi)}\right)\ {\rm I}\left(\frac{1+q}{2-q}, \frac{2\sqrt{z z_0 \xi}}{1-\xi}\right) \end{aligned} \tag{11}$$

[3]According to Aharonian & Atoyan (1996) proton losses above 1 GeV are dominated by nuclear interactions, with a typical lifetime $\tau_{pp} \simeq 6.10^7$ yr / $\left(n/1\,{\rm cm}^{-3}\right)$, so that in a SB where the density is very low τ_{pp} is far longer than the SB lifetime. At the very low end of the spectrum (around the MeV), ionization losses might also come to play. The formalism of Becker, Le, & Dermer (2006) allows for systematic losses, but for mathematical convenience these are supposed to occur at a rate $\propto p^{q-1}$, which can describe Coulomb losses only in the special case $q = 2$.

$$z(p) = \frac{2\,p^{2-q}}{(2-q)\,\sqrt{D_{\rm p}^{\star} t_{\rm esc}^{\star}}}$$

$$\xi(t) = \exp\left(2\,(q-2)\,\frac{D_{\rm p}^{\star} t}{\sqrt{D_{\rm p}^{\star} t_{\rm esc}^{\star}}}\right)$$

where $\mathrm{I}(o,x)$ is the modified Bessel function of the first kind.

4. Superbubbles: Average Cosmic-Ray Spectra

SBs are formed around OB associations by the powerful winds and explosions of massive stars. They are the major hosts of SNRs, and thus major candidates for CR production, as already noted by Montmerle (1979), and investigated by Bykov (2001). SNs in SBs are correlated in space and time, hence the need to investigate acceleration by multiple shocks. The SB interior is magnetized and turbulent, hence the need to evaluate gains and losses due to Fermi 2 and escape between the shocks.

4.1. Method

Our aim is to follow the distribution of CRs produced by SNs inside a SB over the OB association life. For a given cluster, time is sampled by intervals $\mathrm{d}t = 10\ 000$ yr, which is small enough to make sure that at most one SN occurs during that period (but by chance, for big clusters), and which is big enough to consider that the Fermi 1 process has built the CR power-law (2) (acceleration is thought to take place mostly at early SNR stages, and in a SB the Sedov phase starts after a few thousands of years). Here we do not try to investigate the exact extent of the spectrum produced in SNRs: we set the lowest momentum (injection momentum) to $p_{\rm min} = 10^{-2}\,m_p c$ (which is the typical thermal momentum downstream of a SN shock) and we set the highest momentum (escape momentum) to $p_{\rm max} = 10^6 m_p c \simeq 10^{15}$eV (which corresponds to the "knee" break in the CR spectrum as observed on the Earth). Note that the theoretical acceleration time from $p_{\rm min}$ to $p_{\rm max}$ (in the linear regime, without escape) is roughly 8 000 yr (assuming Bohm diffusion with $B = 10\,\mu G$), which is again consistent with our choice of $\mathrm{d}t$. This makes 8 decades in p, with a resolution of a few tens of bins per decade (according to section 2.2.). If no SN occurs in the time bin then the distribution is evolved in time according to (10).

This process is repeated for many random clusters of the same size, until some average trend emerges regarding the shape of spectra. CR spectra are monitored at some reference times, from 5 Myr to 35 Myr by steps of 1 Myr. For a given sample, CR spectra are strongly intermittent during the SB lifetime, especially at early times. Still, we clearly see convergence to an average spectrum as we increase the number of samples. The limit spectrum exhibits a distinctive two-parts shape, with a transition from a hard regime (flat spectrum, slope $s < 4$) to a soft regime (steep spectrum, slope $s \geq 4$). This trend is very robust, but the transition energy depends critically on the SB parameters.

4.2. Parametric Study

For each cluster we have to define 8 parameters: $N_\star, r, q, B, \eta_T, \lambda_{\rm max}, n, x_{\rm acc}$, which are more or less constrained. We sample the size of the cluster roughly logarithmically between 10 stars and 500 stars (the extremal case of Cygnus OB2), ie $N_\star$ =10, 30, 70, 200, 500. We consider only SN shocks[4] of $r = 4$. We compare classical turbulence indexes $q = 5/3$ (Kolmogorov cascade) and $q = 3/2$ (Kraichnan cascade). We consider two different scenarii for the magnetic field: if a turbulent dynamo is at work then $B \simeq 10$ μG and $\delta B \gg B$ so that $\eta_T \simeq 1$ (e.g. Parizot et al. 2004), if not then because of the SB expansion $B \simeq 1$ μG and $\delta B < B$ (if $\delta B = B/2$ then $\eta_T = 0.2$). The external scale of the turbulence $\lambda_{\rm max}$ is at least of the order of the distance $d_\star$ between two stars in the cluster, which, for a typical OB association radius of 35 pc (e.g. Garmany 1994), and assuming uniform distribution (a quite crude approximation), reads $d_\star \simeq 56\,{\rm pc}/N_\star^{1/3}$. But $\lambda_{\rm max}$ can be higher if turbulence is driven by SNRs, the radius of which goes roughly as $r_{\rm SNR} \simeq 38$ pc $\left({\rm t}/10^4\ {\rm yr}\right)^{2/5}$ in the Sedov-Taylor phase inside a SB. Hence we vary $\lambda_{\rm max} = 10, 20, 40, 80\,{\rm pc}$. We take the size of the acceleration region to be of the order of the radius of a SNR after our time-step ${\rm d}t = 10\,000$ yr, that is $x_{\rm acc} = 40$ pc. However in evolved SB it might be higher, up to more than 100 pc, so we also try 80 pc and 120 pc. The typical density of a SB is $n = 5.10^{-3}$ cm^{-3}, to assess its influence we also run simulations with $n = 10^{-3}$ cm^{-3} and $n = 10^{-2}$ cm^{-3}.

Finally we have to set the number N of samplings per cluster: convergence of average spectra typically requires $N_\star \times N \simeq 10\,000$, but the general trend is already clear as soon as $N_\star \times N \simeq 1\,000$, so we simply take $N = 1000/N_\star$.

4.3. Results

After the discussion of last section we had to run 720 different cases. But interestingly enough, it turned out that the effects of the 6 parameters relevant to Fermi 2 and escape $q, B, \eta_T, \lambda_{\rm max}, n, x_{\rm acc}$ can be summarized through a single parameter, the adimensional number $\theta^\star$ introduced by Becker, Le, & Dermer (2006):

$$\theta^\star = \left(D_p^\star\, t_{\rm esc}^\star\right)^{-1} \tag{12}$$

which, according to equations (9) and (7) goes as

$$\theta^\star \propto \eta_T^{-2}\ B^{2q-6}\ \lambda_{\rm max}^{2q-2}\ x_{\rm acc}^{-2}\ n\,. \tag{13}$$

With all the possible SB parameters considered in section 4.2., $\theta^\star$ ranges from 10^{-4} to 10^{+4}. As we consider only strong SN shocks of $r = 4$, the single remaining parameter is the number of stars $N_\star$ (represented through dots of different colors and sizes on the plots), which has a weaker impact on results.

To characterize the CR spectra, we use two indicators, plotted on figure 1. On the left panel we show the momentum of transition from hard to soft regimes, defined as the maximum momentum up to which the slope may be smaller

[4] As SBs are clumpy and turbulent media, many weak secondary shocks ($r < 4$) are also expected, their effect will be studied in a work in preparation.

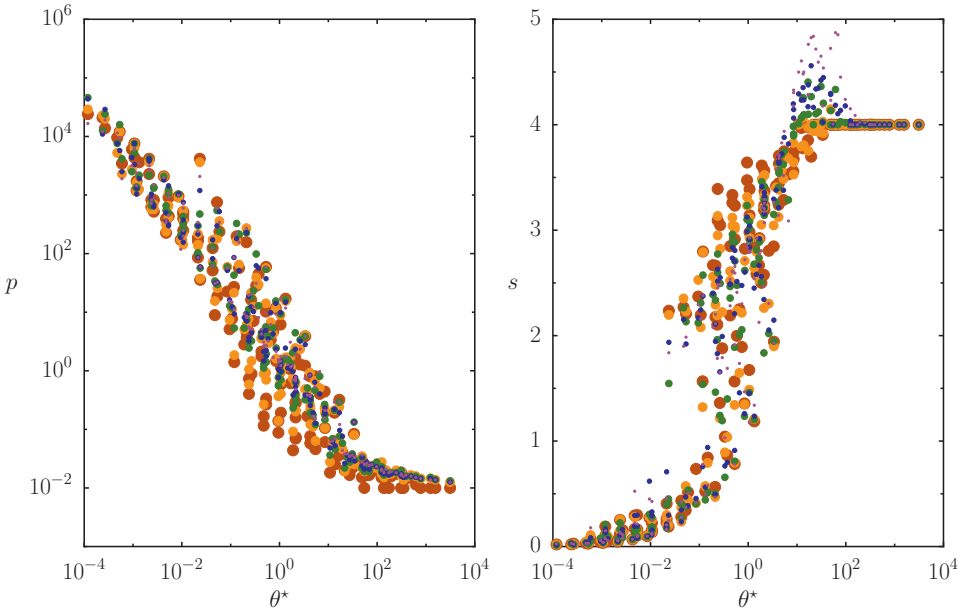

Figure 1. Two indicators of the hard-soft transition as a function of $\theta^\star$. Left: maximum momentum p up to which the slope s may be smaller than 3. Right: lowest slope s obtained at $p = 1$ GeV

than 3 (note that it can happen to be ≥ 3 at a particular time in a particular cluster). On the right panel we show the lowest slope (corresponding to the hardest spectrum) obtained at a fixed momentum of 1 GeV. We see that as $\theta^\star$ rises, *(i)* the transition momentum falls exponentially from almost the maximum momentum considered (a fraction of PeV) down to the injection momentum (10 MeV); and *(ii)* the lowest slope rises from 0 (which is possible with Fermi 2) to 4 (the canonical value of Fermi 1 in the test particle case).

This behaviour can be explained noting that $\theta^\star$ is roughly the ratio of the re-acceleration time and of the escape time. Low $\theta^\star$ are obtained when re-acceleration is faster than escape, allowing Fermi processes to build hard spectra up to high energies, as CRs get re-accelerated by shocks and/or turbulence; high $\theta^\star$ are obtained when escape is faster than re-acceleration, resulting in always quite soft in-situ spectra, as CRs escape immediately after being accelerated by a SN shock. $\theta^\star = 1$ corresponds to a balance between gains and losses, in that particular case the spectral break occurs around 1 GeV.

Conclusion

Our main conclusions are as follows:
(i) CR spectra inside SBs are strongly intermittent (at a given time they depend on the particular history of a given cluster);
(ii) still, CR spectra follow a distinctive overall trend, resulting from a competition between (re-)acceleration by Fermi 1 and Fermi 2 processes and escape:

they are harder at lower energies ($s < 4$) and softer at higher energies ($s > 4$), a shape in agreement with the results of Bykov (2001);
(iii) the momentum at which this spectral break occurs critically depends on the SB parameters: it decreases when the density and the turbulence external scale increase, and increases when the magnetic field value and acceleration region size increase – all these effects being summarized by the single dimensionless parameter $\theta^\star$ defined by (12);
(iv) for reasonable values of SB interior parameters, and especially for highly magnetized and turbulent SBs, very hard spectra ($s < 3$) can be obtained over an important range of CR energies, and at least up to the GeV domain.

These results have important implications on the chemistry inside SBs and the on high-energy emission from SBs. For instance, in the SB Perseus OB2 we have observational evidence for intense spallation activity, attributed to a high density of low-energy CRs, but EGRET has not detected π^0-decay radiation, which puts limits on the density of high-energy CRs. We are looking forward to see how new instruments such as AGILE, GLAST and HESS 2 will perform with such extended sources.

References

Achterberg, A. 1990, A&A, 231, 251
Aharonian, F. A., & Atoyan, A. M. 1996, A&A, 309, 917
Becker, P. A., Le, T., & Dermer, C. D. 2006, ApJ, 647, 539
Blasi, P. 2002, Astroparticle Physics, 16, 429
Bykov., A. M. 2001, Space Sci.Rev., 99, 317
Casse, F., Lemoine, M., & Pelletier, G. 2002, Phys.Rev.D, 65(2), id.023002
Cerviño, M., et al. 2002, A&A, 363, 970
Ferrand, G., Downes, T., & Marcowith, A. 2008, MNRAS, 383, 41
Garmany, C. D. 1994, PASP, 106, 25
Kroupa, P. 2002, Sci, 295, 82
Limongi, M., & Chieffi, A. 2006, ApJ, 647, 483
Malkov, M. A., & Drury, L. O. 2001, Reports on Progress in Physics, 64(4), 429
Melrose, D. B., & Pope, M. H. 1993, Proc. Astron. Soc. Australia, 10, 222
Montmerle, T. 1979, ApJ, 231, 95
Parizot, E., et al. 2004, A&A, 424, 747
Salpeter, E. E. 1955, ApJ, 121, 161